Integrative Metabolomics-Genomics Approach Reveals Key Metabolic Pathways and Regulators of Alzheimer's Disease

Emrin Horgusluoglu, PhD.[1], **Ryan Neff**[1], **Won-Min Song, PhD.**[1], **Minghui Wang, PhD.**[1], **Qian Wang, PhD.**[1], **Matthias Arnold, PhD.**[2,3], **Jan Krumsiek, PhD.**[4], **Beatriz Galindo-Prieto, PhD.**[4,5], **Chen Ming, PhD.**[1], **Kwangsik Nho, PhD.**[6], **Gabi Kastenmüller, PhD.**[2], **Xianlin Han, PhD.**[7], **Rebecca Baillie, PhD.**[8], **Qi Zeng**[1], **Shea Andrews, Ph.D.**[9], **Haoxiang Cheng, PhD.**[1], **Ke Hao, PhD.**[1], **Alison Goate, DPhil.**[9], **David A. Bennett, MD**[11], **Andrew J. Saykin, PsyD**[8], **Rima Kaddurah-Daouk, PhD.**[3,12,13,#], **Bin Zhang, PhD.**[1,#,†], **Alzheimer's Disease Neuroimaging Initiative (ADNI)**[€], **Alzheimer Disease Metabolomics Consortium**[$]

[1]Department of Genetics and Genomic Sciences, Mount Sinai Center for Transformative Disease Modeling, Icahn Institute of Genomics and Multiscale Biology, Icahn School of Medicine at Mount Sinai, NY, USA

[2]Institute of Computational Biology, Helmholtz Zentrum München, German Research Center for Environmental Health, Neuherberg, Germany

[3]Department of Psychiatry and Behavioral Sciences, Duke University, Durham, NC, USA

---

[4]Institute for Computational Biomedicine, Englander Institute for Precision Medicine, Department of Physiology and Biophysics, Weill Cornell Medicine, New York, USA

[5]Helen and Robert Appel Alzheimer's Disease Research Institute, Brain and Mind Research Institute, Weill Cornell Medicine, New York, USA

[6]Center for Neuroimaging, Department of Radiology and Imaging Sciences, Indiana University School of Medicine, Indianapolis, IN, USA

[7]Barshop Institute for Longevity and Aging Studies, University of Texas Health Science Center at San Antonio, San Antonio, TX, 78229, USA

[8]Rosa & Co LLC, San Carlos, California, USA

[9]Department of Neuroscience, Ronald M. Loeb Center for Alzheimer's Disease, Icahn School of Medicine at Mount Sinai, New York, NY, USA

[11]Rush Alzheimer's Disease Center, Rush University Medical Center, Chicago, Illinois, USA

[12]Duke Institute of Brain Sciences, Duke University, Durham, NC, USA

[13]Department of Medicine, Duke University, Durham, NC, USA

Abstract

Metabolites, the biochemical products of the cellular process, can be used to measure alterations in biochemical pathways related to the pathogenesis of Alzheimer's disease (AD). However, the relationships between systemic abnormalities in metabolism and the pathogenesis of AD are poorly understood. In this study, we aim to identify AD-specific metabolomic changes and their potential upstream genetic and transcriptional regulators through an integrative systems biology framework for analyzing genetic, transcriptomic, metabolomic and proteomic data in AD. Metabolite co-expression network analysis of the blood metabolomic data in the Alzheimer's Disease Neuroimaging Initiative (ADNI) shows short-chain acylcarnitines/amino acids and medium/long-chain acylcarnitines are most associated with AD clinical outcomes including episodic memory scores and disease severity. Integration of the gene expression data in both the blood from the ADNI and the brain from the Accelerating Medicines Partnership Alzheimer's Disease (AMP-AD) program reveals *ABCA1* and *CPT1A* are involved in the regulation of acylcarnitines and amino acids in AD. Gene co-expression network analysis of the AMP-AD brain RNA-seq data suggests the *CPT1A* and *ABCA1* centered subnetworks are associated with neuronal system and immune response, respectively. Increased *ABCA1* gene expression and adiponectin protein, a regulator of ABCA1, correspond to decreased short-chain acylcarnitines and amines in AD in the ADNI. In summary, our integrated analysis of large scale multi-omics data in AD systematically identifies novel metabolites and their potential regulators in AD and the findings pave a way for not only developing sensitive and specific diagnostic biomarkers for AD but also identifying novel molecular mechanisms of AD pathogenesis.

Keywords

NARRATIVE

1.1. Contextual background

Alzheimer's Disease (AD) is the most common type of dementia, presently affecting more than 6 million Americans, and the number of AD patients in the US is expected to increase dramatically each year [1, 2]. In the past several decades, many studies have been carried out to investigate CSF biomarkers (Tau and Abeta) [3, 4], neuroimaging measurements of hippocampal/cortical atrophy and amyloid-beta deposition in the brain [5], mitochondrial disturbance [6] and microglial dysfunction and immune response in AD [7] to better understand metabolic alterations in the early stage of AD. Metabolites, which are the biochemical products of cellular processes, can be used as a readout for alterations in biochemical pathways related to the pathogenesis of AD. Despite significant advances in the field, the metabolic basis of AD is, however, still poorly understood, and the relationships between systemic abnormalities in metabolism and AD pathogenesis remain elusive. Similarly, we are still seeking biological processes and genetic mechanisms that might underlie metabolic involvement in AD progression.

The concentration of specific types of metabolites in blood, cells, tissues, and cerebrospinal fluid are influenced by disease pathogenesis [8, 9]. Changes in metabolites have also been linked to genetic variations [10], immune response [11], microbiome [12], and lifestyle and diet [13]. Recent studies revealed that plasma phospholipids were associated with cognitive decline in mild cognitive impairment (MCI) and AD patients [14], and altered sphingomyelin and ceramide levels were observed in the early stage of AD [15]. Furthermore, while glucosylceramides, lysophosphatidylcholines, and unsaturated triacylglycerides levels are significantly associated with cerebrospinal fluid (CSF), Abeta level a monounsaturated sphingomyelins and ceramide levels are positively correlated with CSF total tau and brain atrophy [16, 17]. Acylcarnitines and several amines have been associated with brain volume changes and cognitive impairment in symptomatic stages of AD, while a specific set of sphingomyelins and phosphatidylcholines have been associated with CSF amyloid-beta level in preclinical AD stages [18]. A more recent study revealed that 26 metabolites, including sphingolipids, were highly correlated with hippocampal atrophy, AD-pathology related biomarkers as well as memory scores in the brain and blood in preclinical AD [19].

This study aims to address two critical questions in the metabolomic analysis of AD: (1) "Are metabolite co-expression networks and upstream genetic regulators predictive of disease progression and survival?", (2) "What are the genetic mechanism and upstream regulators of the changes in acylcarnitines and amino acids during AD progression?". We hypothesized specific metabolites are significantly associated with AD-related clinical outcomes, and key genetic drivers play a significant role in regulating metabolites in AD. Towards this end, we systematically interrogated metabolomic, genetic, transcriptomic, proteomic, and clinical data from the matched subjects in the Alzheimer's Disease Neuroimaging Initiative (ADNI) and the metabolomics data generated by the Alzheimer Disease Metabolomics Consortium to identify 1) specific metabolites highly associated with

AD pathology and cognitive phenotypes, 2) key biological processes underlying changes in metabolites in blood.

1.2. Study Conclusions, Future Directions and Limitations

Our results indicate that the balance between essential amino acids/BCAAs and short-chain acylcarnitine homeostasis is disturbed in AD, with medium/long-chain acylcarnitines levels being also significantly different in AD versus control but in the opposite direction. We identified two important genes (*ABCA1* and *CPT1A*) and two proteins (Adiponectin and NGAL) involved in the regulation of acylcarnitines and amines. Increased *ABCA1* gene expression and adiponectin protein (a regulator of ABCA1) corresponded to decreased short-chain acylcarnitines and amines in AD. In addition, *CPT1A* and *ABCA1* genes were differently expressed in the brains of AD patients compared to controls, and their subnetworks were enriched for AD, aging, and neuronal system-related gene signatures/pathways. The proposed framework opens up a new avenue for identifying not only dysregulated acylcarnitine and amine metabolisms in AD, but also genetic mechanisms and biological processes underlying these metabolic changes. We acknowledge that our proposed acylcarnitines/amines hypothesis and the more generic disease-related metabolic perturbation hypothesis derived from integrative analysis of genetic, transcriptomic, proteomic, and metabolomic data are based on a correlation analysis of observed variables. But the advanced network biology approach utilized here has the potential to identify key genes and cellular/molecular pathways that may drive disease-associated perturbations in acylcarnitines, amino acids, and other metabolites. As an example, based on observations for our large-scale integrative analyses, we posit that low levels of the short-chain acylcarnitines/amines and high levels of medium/long-chain acylcarnitines could be highly predictive diagnostic biomarkers for an early stage of AD. Moving forward, we anticipate that machine learning techniques such as random forest and support vector machine (SVM) can be employed to predict disease progression (especially progression towards early AD) using these metabolites [19–21].

However, existing metabolomic and other Omics data represent only a snapshot in time of molecular states of particular patient subpopulations; therefore, network models based on such data should be considered as the initial phase of fully-fledged models, which will be developed from matched, longitudinal multi-Omics data from relatively large patient populations using more advanced network biology approaches such as causal network inference. To further infer causal relationships among a large collection of dissimilar variables at different -omics layers, we can conduct Bayesian probabilistic causal network (BN) analysis [22–25] as we and others have previously done in AD [26–28] and other complex traits [29, 30]. Moreover, the static state BN analysis can be expanded to model dynamic and time-dependent regulation changes in a longitudinal or time-series dataset. For example, a dynamic BN (DBN) framework had been employed to model the dynamic causal network of blood gene expression in response to food intake over multiple time points, where intra-time-slice BN structure from a large data set generated at static states was combined with inter-time-slice structure inferred from the time series data [31]. The data-driven causal networks will provide a systems-wide context for understanding the mechanisms of known regulators and discovering novel key causal

regulators among mRNA, protein, and metabolite levels. As transcription regulates the abundance of metabolites [32, 33], metabolites also transfer the information back to the transcription network directly or indirectly interacting with a transcription factor [34–36].

There are several limitations in our study. First, even though ADNI is one of the best and largest cohorts with matched multi-omics and metabolomics data in AD, we have only a moderate number of metabolites, and we still do not have longitudinal metabolite data to monitor metabolite changes during the course of each individual's disease progression. The other significant limitation is that the transcriptomic and metabolomic data were from the blood. The metabolites in the blood are circulating metabolites and gene expression represents blood cell transcriptomics, and thus, they represent substantially differrent compartments of the body. Such difference limits the findings from our analysis. Another limitation of this study is the lack of an independent cohort to replicate our key findings. Further studies are also needed to validate *ABCA1* and *CPT1A* as potential upstream regulators of acylcarnitines in AD.

One of the major challenges in identifying AD-specific metabolites is that neurodegenerative diseases such as AD, Parkinson's disease (PD), and amyotrophic lateral sclerosis (ALS) have comorbidity. Interestingly, some altered metabolic signatures are common in AD, PD, and ALS [37, 38]. ABC transporters carrying multiple substances through the blood-brain barrier are expressed in all cell types in the brain and are significantly associated with several neurodegenerative diseases [38–40]. Medium/long-chain acylcarnitines, phosphatidylcholine, and lysophosphatidylcholine levels increase in the urine of PD patients [41–43] while plasma levels of acylcarnitine, phosphatidylcholine (PC), and sphingomyelin in AD and MCI patients decreased when compared with healthy individuals [44].

2. CONSOLIDATED RESULTS AND STUDY DESIGN

In this study, we systematically interrogated metabolomic, genetic, transcriptomic, proteomic, and clinical data from the matched subjects in the Alzheimer's Disease Neuroimaging Initiative (ADNI) to identify key drivers and metabolic pathways associated with changes in metabolites with disease severity. We show acylcarnitines and amines are highly correlated with AD clinical outcomes and further reveal key biological drivers and pathways that are involved in metabolomic changes in MCI and AD. One hundred forty metabolites in fasting serum samples from the ADNI (362 controls, 94 with significant memory concerns, 764 with mild cognitive impairment, and 298 with AD), were analyzed using the AbsoluteIDQ-p180 kit. The data were adjusted for age, gender, body mass index (BMI), education, cohort, and medication. A metabolite co-expression network was constructed using Multiscale Embedded Gene co-Expression Network Analysis (MEGENA). Co-expressed metabolite modules were then prioritized by the strength of association with clinical/cognitive and pathological traits. Correlation analysis of the co-expressed metabolite modules and the matched gene/protein expression data was performed. The ROS/MAP cohort was used as a replication study of the co-expression network. Six brain transcriptomic datasets from the Mount Sinai Brain Bank, ROS/MAP, and Mayo clinic cohorts were utilized to build up gene-centered correlation networks to elucidate functions of upstream regulators of candidate metabolites. Modules comprised of short-chain

acylcarnitines/amino acids, and medium/long-chain acylcarnitines were most associated with worse AD clinical outcomes, including episodic memory scores and disease severity. Short-chain acylcarnitines (especially C3), BCAAs (isoleucine and valine) and other amino acids (tryptophan and tyrosine), as well as medium/long-chain acylcarnitines (C12, C14:1/ C14:2, C16:1 and C18), are significantly correlated with AD severity and cognitive traits. *CPT1A* gene expression was highly correlated with an increased level of the medium/ long-chain acylcarnitines. Increased *ABCA1* gene expression and adiponectin (a regulator of ABCA1) protein expression corresponded to decreased short-chain acylcarnitines and amines in AD. In addition, *CPT1A* and *ABCA1* were differently expressed in the brains of AD patients compared to controls, and their subnetworks were enriched for AD, aging, and neuronal system-related gene signatures/pathways. The integration of genetic and transcriptomic data with metabolomic networks, highlights novel pathways and driver molecules that potentially contribute to disease pathogenesis. For example, the interaction between the acylcarnitines and amino acids with proteins such as Adiponectin and NGAL indicates a novel framework of cellular mechanism. In addition, we developed the trajectory inference analysis and Granger causality test on bulk tissue metabolomic data in ADNI using Slingshot [45] to identify metabolite changes along the pseudo time. Preliminary data shows that the expression level of the module of short-chain acylcarnitines and amines decreases over time while that of the module of medium/long-chain acylcarnitines increases over time. Our multiscale metabolite co-expression network of ROS/MAP brain data also revealed that the modules of amines and short-chain acylcarnitine are significantly correlated with neuritic plaque burden in midfrontal cortex, and significantly overlap with the top modules in ADNI. The key strength of our findings in terms of the modeling is that the identification of the biological drivers/pathways highly correlated with the co-expressed metabolites in AD can be used as predictors during disease progression and survival. Integrated analysis of genetic, transcriptomic, proteomic, and metabolomic data pave the way for the development of sensitive and specific diagnostic biomarkers either alone or in combination in the early stage of Alzheimer's Disease.

Our findings clearly indicate that (1) BCAAs and Acylcarnitines are increasingly utilized in AD progression and (2) fatty acid β-oxidation is dysregulated and/or mitochondria are in dysfunction in AD, (3) Acylcarnitines can be predictive of AD phenotype conversion from MCI compared with MCI stable phenotype. Therefore, the results from our correlative study are consistent with the connection between mitochondrial dysfunction and AD pathogenesis but provide more insights into the underlying mechanisms for diabetes as a risk factor for AD. Since previous studies showed increased utilization of branched amino acids is associated with type 2 diabetes and mitochondrial dysfunction is common in diabetes [46, 47], the association of branched-chain amino acids with AD revealed by this study opposite to this notion. Besides the opposite connection between obesity and Type 2 diabetes, elevated medium/long-chain acylcarnitines in plasma are associated with the disruption of β-oxidation in depression [48, 49].

3. DETAILED METHODS AND RESULTS

3.1 Methods

Study Participants

Alzheimer's Disease Neuroimaging Initiative (ADNI): Metabolites in fasting serum samples were obtained from the Alzheimer's Disease Neuroimaging Initiative Phase 1 (ADNI-1) and its subsequent extensions (ADNI-GO/2) for this study (adni.loni.usc.edu). ADNI was launched in 2003 as a public-private partnership, led by Principal Investigator Michael W. Weiner, MD., and participants were recruited from more than 50 sites across the United States and Canada. The ADNI dataset includes serial MRI and PET scans, longitudinal CSF markers, neuropsychological test scores, and clinical assessments. ADNI cohort includes cognitively normal older individuals (CN), significant memory concerns (SMC), mild cognitive impairment (MCI) and AD aged 55–90 (http://www.adni-info.org/). The ADNI dataset includes structural MRI and PET scans, longitudinal CSF markers, and performance on neuropsychological and clinical assessments. Also, ADNI samples have APOE and genome-wide genotyping data, transcriptomics, and whole-genome sequencing data.

Quantitative metabolomics was performed by Alzheimer's Disease Metabolomics Consortium (https://sites.duke.edu/adnimetab/) using ADNI samples and the Biocrates AbsoluteIDQ p180 (Biocrates Life Sciences AG, Innsbruck, Austria) platform. Quantification of serum metabolites including amino acids, acylcarnitines, sphingomyelins (SMs), phosphatidylcholines (PCs), hexoses (h1s), and biogenic amines was done using methods published previously [18, 50, 51]. Flow injection analysis-tandem mass spectrometry (FIA-MS/MS) was used to analyze the acylcarnitines, lipids, and h1s Liquid chromatography-tandem mass spectrometry (HPLC-MS/MS) using an AB SCIEX 4000 QTrap mass spectrometer (AB SCIEX, Darmstadt, Germany) with electrospray ionization was used to analyze the amino acids and biogenic amines. The concentration of each metabolite was measured in μM [18]. Blood metabolites were adjusted for age, gender, body mass index (BMI), education, cohort, and medication information.

We analyzed metabolic profiles from 1,518 individuals, including 362 CN older individuals, 94 individuals with SMC, 270 individuals diagnosed with EMCI, 494 individuals with LMCI, and 298 individuals diagnosed with AD. Supplemental Table S1 includes demographic and clinical characteristics of the ADNI participants.

The Religious Orders Study (ROS) and Rush Memory and Aging Project (MAP): Description of ROSMAP has been previously reported [52]. Metabolomics data from brain ROS/MAP Dataset was used as a replication dataset to test whether metabolite modules are conserved between the blood and the brain (Synapse:syn10235596). Data were obtained with the same Biocrates AbsoluteIDQ p180 kit used in the ADNI study. Brain metabolites (N=163) were adjusted for age, gender, body mass index (BMI), and education. We identified co-expressed metabolite modules from 50 individuals with no cognitive impairment (NCI), 30 individuals with mild cognitive impairment (MCI), 25 individuals

diagnosed with AD. Fisher's exact test (FET) was utilized to test if the co-expressed modules in the blood significantly overlap those from the brain.

Construction of multiscale metabolite co-expression network—We constructed a multiscale metabolite co-expression network (MMCEN) using the quality-controlled and normalized metabolomic data from the blood samples collected from the ADNI participants (N=1,518). The Biocrates AbsoluteIDQ p180 platform, which measures amino acids, acylcarnitines, sphingomyelins (SMs), phosphatidylcholines (PCs), hexoses (h1s), and biogenic amines, was used to generate the metabolite data [53]. In total, 140 metabolites were used in the metabolite network analysis. The metabolite expression data from 1,518 individuals were adjusted for age, gender, body mass index (BMI), education, and cohort (ADNI1 and ADNIGO/2).

A metabolite co-expression network for the ADNI blood expression data was constructed using Multiscale Embedded Gene co-Expression Network Analysis (MEGENA) [54]. MEGENA first constructed a Planar Filtered Network (PFN) from significantly correlated metabolite pairs of the resulted PFN then went through a multiscale clustering analysis to identify co-expressed modules using different scales of compactness of modular structures controlled by a resolution parameter. The metabolite modules were then compared with random PFN modules generated by shuffling the link weights of the parent cluster to calculate the statistical significance of each module. A multiscale hub analysis was then performed to identify highly connected hub nodes (metabolites) for each significant module. The modules with less than 10 metabolites were excluded from further downstream analyses. Finally, principal component (PC) analysis was performed on each module to obtain the principal component vectors (eigen-metabolites) for subsequent correlation analysis of modules and various cognitive, clinical and neuropathological traits.

Cognitive and neuropathological traits—AD-pathology related traits including Clinical Dementia Rating Sum of Boxes (CDR-SB), cerebrospinal fluid tau, phospho-tau (p-tau) and amyloid-beta levels, Fluorodeoxyglucose (18F) (FDG)-PET, Florbetapir (AV-45) PET, clinical and cognitive performance data, were downloaded from the ADNI1 and ADNIGO/2 database (http://adni.loni.usc.edu). CSF measurements and quality control data were obtained from the LONI website as "UPENN CSF Biomarkers Elecsys." The complete descriptions of the collection and process protocols can be found at www.adni-info.org. Alzheimer's Disease Assessment Scale (ADAS-Cog), Mini–Mental State Examination (MMSE), Rey Auditory Verbal Learning Test (RAVLT), and Montreal Cognitive Assessment (MoCA) scores and self (PT)- and informant (SP)- everyday cognition (ECog) memory scores which include language, visuospatial, organization of items and divided attention were downloaded as representations of cognitive test scores [55–57]. Rey Auditory Verbal Learning Test (RAVLT) score, the assessment of episodic memory, consists of 5 learning trials of 15 words, immediate recall, and 30-minute delayed recall, as well as an interference list and recognition test. MMSE and MOCA measures memory, recall, and attention [58]. The other important memory score is ADAS-Cog, which is similar to RAVLT and measures the episodic memory using ten unrelated words. For all score types, those scores determined baseline was chosen for our analyses. Since not all participants in ADNI have cognitive,

clinical, and pathology recorded scores, Supplemental Table S2 summarizes how many participants were included for each correlation-based analysis.

Correlation analysis of the metabolite modules and neuropathological traits—
To determine the predictive power of the co-expressed metabolite modules of the MMCEN, we evaluated correlations of the metabolite modules with clinical/cognitive CSF (tau and Aβ) and imaging (FDG and AV45 PET) biomarker variables. We ranked order co-expressed metabolite modules based on the overall strength of such correlations. Since each module includes at least ten metabolites, we reduced the dimensionality of the data by computing the first principal component (PC) from the metabolites in each module and then computed Spearman's correlation coefficient r_{ij} between each clinical/cognitive/CSF trait (i) and the first PC of each metabolite module (j). P-value (P_{ij}) of the correlation coefficient r_{ij} was computed via the asymptotic t approximation. Significant correlations were defined as those with multiple testing adjusted P value less than 0.05 (adjusted by the $i*j$ number of correlations).

The aforementioned correlations between a metabolite module (j) and clinical/cognitive/ pathological traits were then combined into a composite importance score by $S_j = \frac{1}{n}\sum_i |r_{ij}|$, where n denotes the total number of traits. The importance score essentially computes the mean of the absolute value of the correlation coefficients across traits for each metabolite module. We have previously used this type of composite score to rank order the importance of key driver genes identified in gene networks across multiple brain regions [26]. The metabolite modules were then ranked by their composite importance scores. All available clinical/cognitive/AD-pathological traits were used for the correlation analysis.

Identification of genes correlated with metabolite co-expression network—
Microarray-based RNA gene expression data from blood samples of 745 ADNI participants was downloaded from the ADNI LONI website (http://adni.loni.usc.edu) [59]. We only included the individuals with both metabolomic and transcriptomic data (N=417; CN=121, EMCI=183, LMCI=76, AD=37). Probe sets of the Affymetrix Human Genome U219 platform (Affymetrix, Santa Clara, CA) were excluded from the data if they did not match any gene or matched multiple genes. All gene expression data were adjusted for RIN, batch effect, and sex. For each gene with multiple probes, the probe with the most variation across all the samples was selected as the representative of the gene. In total, 17,848 genes were included in the correlation analysis of the gene expression data and the metabolite modules using both Pearson and Spearman correlation analyses. Significance levels were adjusted by multiple testing. Adjusted p <0.05 was considered statistically significant for all the analyses carried out in this study.

Construction of *CPT1A* and *ABCA1* centered co-expression gene network in AD—Six RNA-seq datasets from six different brain regions in three human postmortem brain cohorts, including the Mount Sinai Brain Bank AD cohort (MSBB) (4 cortical regions) [60], the Religious Order Study (ROS) and the Rush Memory and Aging Project (MAP) (ROSMAP) cohort (the dorsolateral prefrontal cortex (DLPFC)) [61, 62] and the Mayo

Clinic cohort (the temporal cortex (TCX)) [63] were used for constructing *CPT1A* and *ABCA1* centered co-expression gene networks.

The MSBB AD cohort contained brain specimens obtained from the Mount Sinai/JJ Peters VA Medical Center Brain Bank, which holds over 1,700 samples. This cohort was assembled after applying stringent inclusion/exclusion criteria and represents the full spectrum of disease severity ranging from cognitively normal to severe dementia. RNA-sequencing gene expression profiles were generated across four cortex brain regions (the frontal pole, the superior temporal gyrus, the parahippocampal gyrus, the inferior temporal gyrus) from about 360 brains [60]. Besides, microarray gene expression data were also generated from a smaller set of brains for 19 different cortical regions, including the hippocampus of 55 brains, which was used here [64]. The ROSMAP dataset included two prospective cohort studies of aging as the Religious Order Study (ROS) and the Rush Memory and Aging Project (MAP) [52, 65]. About 60% of the subjects had a pathologic diagnosis of AD at autopsy. ROSMAP has postmortem RNA-sequencing data generated from the DLPFC of over 600 brains [65]. The preprocessed expression data for the MSBB AD RNA-seq and ROSMAP RNA-seq cohorts were downloaded from the AMP-AD knowledge portal at Synapse [66]. The Mayo RNAseq Study includes whole transcriptome data for 274 temporal cortex (TCX) samples from North American Caucasian subjects with a neuropathological diagnosis of AD, progressive supranuclear palsy (PSP), pathologic aging (PA) or elderly controls (CON) without neurodegenerative diseases. For each dataset, we calculated correlation coefficients between each candidate gene (*CPT1A* or *ABCA1*) and the rest genes. We only focused on the genes present in all the six gene expression datasets. Finally, the genes showing significant correlations with *CPT1A* and *ABCA1* (FDR-corrected p values 0.05) in all the six datasets with consistent correlation direction were used to define the *CPT1A*-centered and *ABCA1*-centered correlation networks, respectively.

Identification of proteins correlated with metabolite co-expression network —The proteomic data of 146 proteins in the RBM Human DiscoveryMAP panel from 566 participants at the baseline visit from the ADNI-1 dataset were downloaded from the ADNI official website (http://adni.loni.usc.edu). Sample selection criteria and quality control steps were explained previously [67]. The data were adjusted for age and sex. Four hundred ninety-eight (498) individuals (CN=51, MCI=343, and AD=104) with both blood metabolomic and proteomic data were used for this analysis. In the module-protein correlation analysis, the first PC of each metabolite module was used for computing correlation with each protein. Both the Pearson and Spearman correlation analyses were performed, and significance levels were corrected for multiple testing. An adjusted p-value <0.05 was considered statistically significant.

Mendelian Randomization Analysis—Summary-data-based Mendelian Randomization (SMR) [68, 69] and Heterogeneity In Dependent Instruments (HEIDI) tests were conducted to explore likely causal paths that link gene expression to metabolite concentrations. We integrated summary statistics from our metabolites GWAS and GTEx v7 eQTL summary data [70], GTEx-brain eQTL summary data [71], Cardiogenics study [72, 73], eQTLGen Consortium [74] and eQTL ADNI blood.

Input/output of each experimental steps and study workflow can be found in Supplementary Figure S1.

Major Computational Tools Analyzing and Integrating Metabolomics and Other Types of Omics Data—This study utilized several major computational tools, including data preprocessing and imputation, Mendelian Randomization, and metabolite co-expression network analysis. The metabolomics data was preprocessed to limit the potential for false-positive findings. To this end, missing values were imputed using minimum value imputation (half of the plate-specific limit of detection), single measurement outliers were winsorized to 3 standard deviations from the global mean, and multi-variate sample outliers were removed using Mahalanobis distance. The imputation had no significant influence on metabolite associations with AD biomarker profiles [75]. We used SMR [76] for Mendelian Randomization to investigate pleiotropic relationships between the expression level of a gene and disease risk. This method effectively tests whether the effect size of an SNP on a phenotype is mediated by gene expression and uses a heterogeneity test (HEIDI test) to distinguish pleiotropy from the linkage. However, it is important to note that statistical analyses such as HEIDI or COLOC [77] are not capable of providing perfect separation of pleiotropy and linkage [68], are dependent on the tissue-specific effect of eQTLs, and to date predominantly utilize cis-eQTLs and exclude trans-eQTLs. The proposed metabolite co-expression network analysis aims to systematically identify co-expression and co-regulation relationships among metabolites. The high complexity of co-expression and co-regulation structures requires effective analytic algorithms to uncover the natural network organization of metabolite-metabolite interaction, such as modularity and hierarchy among the modules. MEGENA can identify biologically more meaningful and relevant co-expressed metabolite clusters than previously established network clustering methods such as eigenvector spectral clustering and WGCNA [54]. However, some true correlations may be missed in an MEGENA derived network due to the application of a planarity constraint. In addition, the co-expression network analysis doesn't explicitly define causal relationships though hub nodes are more likely to be key regulators.

3.2 Results

3.2.1 A multiscale metabolite co-expression network (MMCEN) revealed that Acylcarnitines and Amines are highly associated with AD worse outcomes in blood—By combining two ADNI cohorts (ADNI1 and ADNIGO/2) (Supplemental Table S1) in this study provides further evidence that short-chain acylcarnitines (especially C3), BCAAs (isoleucine and valine) and other amino acids (tryptophan and tyrosine), as well as medium/long-chain acylcarnitines (C12, C14:1/C14:2, C16:1 and C18), are significantly correlated with AD severity and cognitive traits (Supplemental Table S2). First, we identified co-expressed metabolites as modules through the multiscale embedded gene co-expression network analysis (MEGENA) [54] of the metabolomic data in the ADNI, and eleven co-expressed metabolite modules were identified (Figure 1A; Supplementary Table S3). Note that the metabolomic data were corrected for age and other covariates (Methods) and thus the results from the subsequent analyses of the data are independent of age. Multiscale in MEGENA means multiple levels of clustering compactness used for identifying clusters or modules with a hierarchical structure. Metabolite modules are then characterized and

prioritized by association with AD through correlation analysis of the first principle component of each metabolite module and various clinical/cognitive/AD-pathology traits (Figure 1B–C). The top-ranked metabolite modules include short-chain acylcarnitines (C0, C3, and C5) and amino acids (histidine, lysine, tryptophan, asparagine, isoleucine, tyrosine, alanine, arginine, proline, valine, tyrosine, sarcosine, serotonin sarcosine, serotonin) as well as medium/long-chain acylcarnitines (C5.DC..C6.OH., C6..C4.1.DC., C7.DC, C8, C9, C10, C10.2, C12, C14.1, C14.1.OH, C16, C16.1, C18, C18.1) (Supplementary Table S4). To better understand which metabolites significantly changed during disease progression (CN → SMC → EMCI → LMCI →AD), univariate analysis of variance was performed on individual metabolites using SPSS 23.0. Propionylcarnitine (C3), valerylcarnitine (C5), histidine (His), lysine (Lys), tryptophan (Trp), valine (Val), sarcosine in the top module M8 showed the most significant decrease during the course of disease progression, which was also confirmed by the down-regulation in the MCI and AD groups (p-value < 0.05). On the contrary, five important medium/long-chain acylcarnitines as C12, C14.1, C14.2, C16.1, and C18 in the module M6 significantly increased in the blood during the course of disease progression (C12: Dodecanoylcarnitine; C14.1: Tetradecenoylcarnitine; C14.2: Tetradecenoylcarnitine; C16.1: Hexadecenoylcarnitine; C18.1: Octadecenoylcarnitine). Interestingly, the C18 level significantly increased in the LMCI group compared with CN.

In addition, we compared the module and metabolite expression levels in the MCI-to-AD converters with those in the MCI non-converters. The module M6 includes medium/long-chain acylcarnitines, which significantly increased in the MCI-to-AD converters compared with MCI stable individuals over two years (p=0.016) (Figure 2), suggesting medium/long chain acylcarnitines as risk factors for AD. We also developed a multiple logistic regression model to predict MCI to AD pheno-conversion status (0=non-converter, 1=converter) using multiple predictors including network modules, metabolites, clinical traits, and imaging features based on the ADNI cohort. To validate our model, we used 10-fold cross-validation on the 368 participants (converters=104, non-converters=264) with all the predictors available and determined the mean precision, recall, and accuracy across all the runs. Prediction yielded a continuous value from 0 to 1, converted to a binary prediction of conversion status using a cutoff value of 0.35. Our logistic model used the following variables to predict MCI conversion status: M6, M10, M11, M12, M21, education, ADAS13 (baseline), MMSE (baseline), RAVLT (baseline), Hippocampal volume (baseline), C3, C18, C14.1, and C14.2. We achieved an average accuracy of 76.88% (std=7.53%) in 10-fold cross-validation. To predict continuous hippocampal and whole brain volumes at two years (24 months) post-baseline measurement, we developed a generalized linear model using the same predictors for MCI conversion status and intracranial volume (ICV) at baseline as an additional covariate. Model accuracy from 10-fold cross-validation was determined by assessing the Pearson correlation between predicted and observed hippocampal and whole brain volumes for all participants. We achieved a Pearson correlation R^2 of 0.938 (p-value= 2.15×10^{-223}) for the hippocampal volume and 0.694 (p-value=4.46×10^{-96}) for the whole brain volume at 24 months.

3.2.2 Acylcarnitines and Amines are significantly associated with AD-pathology in brain—To examine the concordance between blood and brain metabolites

in AD, we constructed the multiscale embedded gene co-expression network analysis using The ROSMAP brain metabolite data (CN=50, MCI=30, and AD=25) and then rank-ordered metabolite modules by the strength of correlation with AD endophenotypes such as memory scores and neurotic plaque burden. The top three modules (M10, M3, and M17) (Supplementary Table S5) contain short-chain acylcarnitines and Amines, and are significantly correlated with neuritic plaque burden in midfrontal cortex (FDR corrected p-value = 0.03) (Supplementary Table S6). Interestingly, the top metabolite module in the blood metabolite network significantly overlaps the top one in the brain metabolite network, and both modules contain short-chain acylcarnitines and Amines (representation factor: 3.7 $p < 2.8 \times 10^{-6}$). Therefore, the analysis shows that the metabolomic changes in the blood and the brain could be early biomarkers of AD.

3.2.3 Co-Expression Metabolite Transcriptome Network Analysis establishes a link between metabolites and a blood transcriptional network associated with AD—We then integrated the metabolomic and transcriptomic data from the blood of ADNI participants at the baseline visit to identify potential genes associated with the eleven metabolite modules. Based on the data from the participants with both transcriptomic and metabolomic data (CN=121, MCI=259, AD=37), we identified ten genes highly correlated with the top three modules containing short-chain acylcarnitines and amino acids (M8 and M3) as well as medium/long-chain acylcarnitines (M6) (Table 1). After our novel finding in the blood data, we further examined the expression levels of those eight genes in the brains of the subjects with or without AD using the MSBB (4 cortex regions) [60] and Mayo Clinic (DOI:10.7303/syn5550404) cohorts. Two of the eight genes (*CPT1A* and *ABCA1*) are differentially expressed between AD and control in the parahippocampus gyrus (PHG) from the MSBB AD cohort and the temporal cortex (TCX) from the Mayo Clinic cohort with FDR corrected p-values = 3.06×10^{-4} and 1.35×10^{-4}, respectively (Table 2). Our correlation analysis shows that *CPT1A* is significantly associated with a medium/long-chain acylcarnitine enriched module. C12, C14.1, C14.2, C16, and C18 acylcarnitines levels increase in MCI and AD group compared with cognitively healthy individuals. In addition, *CPT1A* is differentially expressed in the PHG and the TCX of the AD subjects compared with the normal control. *CPT1A*-dependent regulation of acylcarnitines transfer may control the levels of C12, C14.1, C14.2, and C16 as well as C18 in the plasma during disease progression. As the accumulation of medium/long-chain fatty acylcarnitines is associated with AD development and progression, fatty acid transport into mitochondria becomes critical. Since fatty acid transport through *CPT1A* is the limiting step of this transport process, the connection of *CPT1A* gene/protein expression with AD becomes obvious. This finding suggests that *CPT1A* may serve as a drug target for the accumulation of fatty acylcarnitines and thus for AD.

Carnitine is essential for the transport of the long-chain acyl-CoAs into mitochondria, which are converted to acylcarnitines by carnitine palmitoyltransferase 1 (CPT1) [78, 79]. There are three forms of CPT enzyme including CPT1A, CPT1B, and CPT1C [80]. CPT1 activity has been implicated in several neurodegenerative diseases as a relationship with the alteration of insulin equilibrium in the brain [81]. The regulation of CPT1 affects the limited levels of long-chain acylcarnitines as C16-, C18-, and C18:1-CN levels that

lead to the increase of free-CN:C16-CN in the plasma [82]. Increased plasma levels of C14:1-CN and C16-OH–CN have bene identified as a product of very-long-chain acyl-CoA dehydrogenase and long-chain 3-hydroxyacyl-CoA dehydrogenase, respectively during β-oxidation in obesity and Type 2 diabetes [82]. Similarly, we identified *CPT1A* is significantly associated with a module comprised of medium/long-chain acylcarnitines. C12, C14.1, C14.2, C16, and C18 acylcarnitine levels increase in MCI and AD group compared with cognitively healthy individuals. Furthermore, *CPT1A* was differentially expressed in the hippocampus and the temporal cortex of the AD subjects compared with the normal control. We may conclude that *CPT1A*-dependent regulation of acylcarnitine transfer may control the levels of C12, C14.1, C14.2, and C16 as well as C18 in the plasma during disease progression. Acylcarnitine levels with mitochondrial fatty acid β-oxidation significantly increases in patients with major depression because of the metabolic dysfunction [49], and the association of medium/long-chain acylcarnitines with AD revealed by this study shows the same of this notion. Anti-depressants that decrease acylcarnitine levels in major depression patients might be considered for a potential treatment for AD patients.

We also show that *ABCA1* gene expression is negatively correlated with the module M8 comprised of short-chain acylcarnitines and amino acids. While the levels of the metabolites in M8 significantly decrease in AD, *ABCA1* expression in the blood increases in the AD group compared with the other groups. *ABCA1* belongs to the superfamily of ATP-binding cassette proteins and plays a vital role in stimulating the efflux of cellular cholesterol from macrophages to Apolipoprotein A-1 (ApoA-1) and HDL, respectively [83–86]. It has been shown that the *ABCA1* gene expression increased in the CA1 region of the hippocampus in AD compared with healthy control [87]. *ABCA1*, which is highly expressed in the brain, plays an essential role in the lipidation of AD risk gene Apolipoprotein E (ApoE) and enables clearance of amyloid-beta accumulation [88, 89]. Our *ABCA1* centered consensus co-expression network demonstrates a strong interaction between *ABCA1* and *APOE* in the brain. Since the module M7 consisting of glycerophospholipids (mostly Lysophosphatidylcholines) is highly correlated with the reduction of the short-chain acylcarnitine and amino acid modules (M8 and M3) and *ABCA1* level, our finding may suggest that *ABCA1* blood expression level increases as a compensation to the reduction of the glycerophospholipids.

In addition to our finding of the increased level of long-chain acylcarnitines in MCI and AD, we detected a significant decrease in the metabolite module containing C3 and amino acids in the MCI and AD groups. Acylcarnitines are produced explicitly in mitochondria using different substrates. Acylcarnitines containing eight or more carbon atoms are generated from the fatty acid β-oxidation; short-chain acylcarnitines (i.e., C3 to C6) are yielded from further β-oxidation as well as oxidation of amino acids; and C2 acylcarnitine is from all the energy substrates including fatty acids, amino acids, and glucose. Among short-chain acylcarnitines, odd-numbered acylcarnitines (i.e., C3 and C5) are specifically generated from BCAAs, suggesting BCAA/short-chain acylcarnitines are linked biochemically and functionally [82, 90]. Decreased levels of C3 in MCI compared with healthy individuals [91] and a distinguished level of C3 metabolite identified in the inferior temporal gyrus in the AD brain were reported previously [19]. We show that *ABCA1* gene expression is negatively correlated with the short-chain acylcarnitine and amino acid module (M8) and differentially

expressed in AD versus CN. We further reveal that the Adiponectin level, which controls *ABCA1* expression through liver X receptor alpha (LXRα) in macrophages in the liver [92], is highly correlated with the short-chain acylcarnitines and branched-chain amino acids. Since *RXRA* mRNA level is highly correlated with that of *ABCA1* in the brain, changes in the mRNA level of RXR/LXR (transcription factors) might upregulate *ABCA1* in AD. *ABCA1* overexpressed AD mice might be used to validate this hypothesis.

Summary-data-based Mendelian Randomization (SMR) and Heterogeneity In Dependent Instruments (HEIDI) tests were conducted [68, 69] to explore likely causal paths that link *ABCA1*/*CPT1A* gene expression to metabolite (C3, C5, His, Lys, Trp, Val, Sarcosine, C12; C14.1; C14.2; C16.1; C18.1) concentrations. To accomplish this, we integrated summary statistics from our metabolites GWAS and GTEx v7 eQTL summary data [70], GTEx-brain eQTL summary data [71], Cardiogenics study [72, 73], eQTLGen Consortium [74] and eQTL ADNI blood. cis-eQTLs were significantly associated with *ABCA1* and *CPT1A* expression in human monocytes and macrophages in Cardiogenics study (NSNP_ABCA1= 19, NSNP_CPT1A = 1991), human Brain in GTEx v7 eQTL study NSNP_ABCA1= 49, NSNP_CPT1A = 1, and the ADNI blood (NSNP_ABCA1= 23, NSNP_CPT1A = 17). However, SMR/HEIDI analysis did not identify a causal path between *ABCA1* and *CPT1A* gene expression and metabolite concentrations. In the blood, *MRPL47* was identified as the most likely gene whose expression levels were associated with C3 and histidine metabolite levels because of causality/pleiotropy at the same underlying causal variant (rs10513761) while *SLC22A5* was highly associated with C14.1, C14.2, and C18.2 metabolite levels because of causality/pleiotropy at the same underlying causal variant (rs2631360) (SMR-multi corrected p-value < 0.05; Supplementary Table S7).

It is important to note that the presumptive mechanism proposed by this study is essentially based on a set of 'correlations', which may or may not indicate causative linkages among the observed variables. Further animal model studies would help to understand the causative linkage between genes/proteins and metabolites. For example, *ABCA1* is not only a key factor for ApoE particle lipidation in the brain, as discussed above, but also plays a crucial role in cholesterol and phospholipid homeostasis in the whole body. Therefore, it is expected that *ABCA1* has many functions involving the cellular membrane and subcellular organelles. The association of *ABCA1* with PC and lysoPC species revealed in the study clearly indicates such a connection. Further investigation is needed to determine whether alterations in phospholipid homeostasis induced by ABCA1 expression and Adiponectin lead to changes in general mitochondrial function, which subsequently affect energy metabolism and substrate utilization. The importance of *ABCA1* beyond the lipidation of ApoE particles in the brain and association with AD pathogenesis should be recognized using the transgenic *ABCA1* mice model. We could measure the levels of acylcarnitines, BCAA as well as phosphatidylcholine and cholesterol efflux from *ABCA1* expressing cells and APOE lipidation ex vivo. Since *ABCA1* is upregulated in AD brains, compared with control, the measurement of metabolites and their upstream regulators in *ABCA1* overexpressed mice would help us identify the mechanism between *ABCA1* and short-chain acylcarnitines and lysophosphatidylcholine.

There are some tool compounds available to explore ABCA1 and CPT1A involved pathways. Multiple HDL apolipoproteins, including apolipoproteins A-I and A-II, interact with ABCA1 and activate multiple signaling pathways such as Janus kinase 2/signal transducer and activator of transcription 3 (JAK2/STAT3), protein kinase A, Rho family G protein CDC42, and protein kinase C [93]. The activation of protein kinase A and Rho family G protein CDC42 involve in the regulation of ABCA1-mediated lipid efflux, and JAK2/STAT3 regulates both ABCA1-mediated lipid efflux and anti-inflammation [93]. Liver X receptors (LXR) and Retinoic X Receptors (RXR) are the other regulators of *ABCA1* transcription [94]. Bexarotene, an FDA-approved RXR agonist, decreases amyloid-beta plaque accumulation and cognitive impairment, and increases amyloid-beta clearance in mice [95–98]. On the other hand, Etomoxir, an inhibitor of CPT1A, is a small molecule that prevents fatty acid oxidation, and induces oxidative stress [99]. Etomoxir inhibits the formation of acyl-carnitine and the transport of fatty acyl-CoA into the mitochondria and is an efficient CPT1A blocker to treat anhedonia and inflammation in depression [100]. The effectiveness of these compounds for treating AD need be further investigated.

Besides animal models, induced pluripotent stem cells (iPSCs) provides an excellent opportunity to identify fatty acid metabolism associated genes and their upstream regulators during the beta-oxidation in AD [101, 102]. Since long-chain fatty acids could not diffuse the mitochondrial inner membrane without the carnitine palmitoyltransferase (CPT) 1, translocase, and CPT2 during fatty acid breakdown [103], we could use the fatty acid oxidation-related metabolites to the induction of iPSCs to better understand how the reaction mediated by CPT1A and CACT (Carnitine/Acylcarnitine Translocase) is disturbed during the disease progression. iPSC-based model systems and CRISPR/CAS9 gene editing of iPSCs [102] will be critical in understanding the roles of *CPT1A* and *ABCA1* as well as their variations/mutations may modify AD risk. We could investigate the essential metabolites and factors required for the formation of pathology using a human brain tissue model from iPSC cells [102, 104]. While iPSCs are stripped of their aging brain epigenome, there are strong polygenic risk associations with AD and related dementia traits [105–107]. The polygenic risk approach using the novel AD candidate genes identified here will help us define the experimental models and systems to test the associated metabolites.

3.2.4 *ABCA1* and *CPT1A* centered gene co-expression subnetworks are enriched for AD signatures—To understand the functional contexts in which *CPT1A* and *ABCA1* operate in AD, we construct *CPT1A* and *ABCA1* centered gene co-expression networks using six gene expression datasets from six different brain regions in three AD cohorts of human postmortem brains, including the Mount Sinai Brain Bank (MSBB) AD cohort (4 cortical regions) [60], the ROSMAP RNA-seq (DLPFC) [61, 62] and the Mayo Clinic cohort (TCX) [63] (Supplemental Table S8). *CPT1A* is positively correlated with 765 genes and negatively correlated with 621 genes (Figure 3A–C; Supplementary Table S9), while *ABCA1* is positively correlated with 675 genes and negatively correlated with 806 genes) (Figure 4A–C; Supplementary Table S10) in all six datasets (FDR corrected p-value $< 10^{-6}$). The *CPT1A-centered* subnetwork is enriched for AD signatures and neuronal system-related pathways such as synapse, synapse part, neuron part, metabolic process, synaptic signaling, neurogenesis and immune system (Figure 3B–D; Supplementary Table

S11–S12). The *ABCA1* centered subnetwork is enriched for known AD gene signatures and pathways such as immune system, neuron part, tyrosine kinase signaling, metabolic syndrome, synaptic signaling, and metabolic process (Figure 4B–D; Supplementary Table S13–S14).

Co-Expression Metabolite Protein Network Analysis establishes a link between metabolites and protein network associated with AD: Since ABCA1 plays an important role in cholesterol and phospholipid transport and *ABCA1* gene expression is controlled by Adiponectin, an adipocyte-specific protein [92, 108, 109], we hypothesize that Adiponectin is highly correlated with the level of module M8 (short-chain acylcarnitine and amino acids). In ADNI-1, 496 individuals (CN=49, MCI=343, AD=104) had both metabolomic and proteomic data (N=146 proteins). Our correlation analysis reveals that Adiponectin is significantly correlated with the modules M8 and M3 with corrected p-value = 0.012 and 0.013, respectively. Moreover, we identify several key proteins that are highly correlated with medium/long-chain acylcarnitines (FDR < 0.05) (Table 3). However, Neutrophil Gelatinase Associated Lipocalin (NGAL), Hepatocyte Growth Factor (HGF), Thrombomodulin, Leptin, Myoglobin, Ferritin, and AXL Receptor Tyrosine Kinase (AXL) are among the proteins highly correlated with medium/long-chain acylcarnitine module (M6). Since Adiponectin has been shown to play an essential role in the regulation of *ABCA1* expression [92] and be correlated with AD [110], we test if *ABCA1* gene expression and Adiponectin levels changed similarly across diagnosis groups. Opposite to the decrease of the short-chain acylcarnitines and amino acids in M8 in the AD group (Figure 5A), *ABCA1* mRNA expression and adiponectin levels increase in the AD patients compared with cognitively normal individuals (Figure 5B–C). Our finding suggests interactions among *ABCA1*, Adiponectin, short-chain acylcarnitines and amino acids in AD. NGAL is the other interesting finding highly correlated with our medium/long-chain acylcarnitine module (M6). Both the metabolites in M6 (Figure 6A) and NGAL (Figure 6B) increase in AD, comparing the cognitively normal group (p-value < 0.05).

Adiponectin is released from the adipose tissue as a hormone and is associated with many cardiovascular and neurodegenerative diseases [111]. Adiponectin has a protective effect on oxidative stress due to amyloid-beta accumulation in the brain [112]. Adiponectin is a key hormone in the regulation of energy metabolism and fatty acid homeostasis and plays a key role in the development of diabetes/obesity and the modulation of brain insulin balance and amyloid-beta in the early stage of AD [111, 113]. The connection of short-chain acylcarnitines with this gene and other related ones is obvious. Modulating adiponectin expression to reduce short-chain acylcarnitine production and accumulation could be important in both diabetes and AD. Adiponectin, as a potential drug target for the treatment of diabetes, has been well recognized. Thus, Adiponectin, which serves as a potential candidate for the treatment of AD, could also be considered. Our integrative analysis of metabolomic, transcriptomic, and proteomic data revealed decreased short-chain acylcarnitines and amino acids and increased *ABCA1* mRNA and Adiponectin protein levels in AD comparing cognitively healthy group. This novel result may suggest that the increase of circulating adiponectin levels and *ABCA1* expression could be a compensatory effect

against neurodegeneration. *ABCA1* overexpressed mice model would help us to understand the upstream regulators and biological processes better.

Conclusion—This report represents emerging novel evidence of metabolic network failures related to AD pathology. A new perspective for prevention and treatment of AD involves key genetic drivers and pathways underlying metabolomic changes in the blood by integrating metabolomic, genetic, transcriptomic, and proteomic data in AD. This effort aims to reassess the role of acylcarnitines and amines, and their potential upstream genetic and transcriptional regulators through this highly integrative analysis of multi-omics data in AD, which paves the way for identifying novel biomarkers as well as therapeutic targets for AD. Detection of changes of small molecule metabolites in blood, cells, tissues, and cerebrospinal fluid at the early stage of AD is challenging but would help us to understand the metabolic mechanisms underlying AD. Metabolite-based biomarker studies enable us to interpret the elusive pathophysiology of neurodegenerative diseases. AD is a heterogeneous disorder associated with multiple clinical and pathological phenotypes as well as many genetic risk factors. Unraveling the heterogeneity of AD will pave the way for not only understanding the mechanisms of AD but also developing novel therapeutics. For this consideration, a future direction is to identify AD subtypes using metabolomic data.

In conclusion, the identification of acylcarnitines enriched modules and their potential upstream genetic and transcriptional regulators through this highly integrative analysis of multi-omics data in AD paves the way for identifying novel biomarkers as well as therapeutic targets for AD. Our novel findings may suggest that an increase of circulating adiponectin and metabolite dependent *ABCA1* mRNA expression could be a compensatory effect against neurodegeneration.

Supplementary Material

Refer to Web version on PubMed Central for supplementary material.

Acknowledgement

References

1. Shen L, et al. , Genetic analysis of quantitative phenotypes in AD and MCI: imaging, cognition and biomarkers. Brain Imaging Behav, 2014. 8(2): p. 183–207. [PubMed: 24092460]

2. Alzheimer's A, 2016 Alzheimer's disease facts and figures. Alzheimers Dement, 2016. 12(4): p. 459–509. [PubMed: 27570871]

3. Zetterberg H, Wahlund LO, and Blennow K, Cerebrospinal fluid markers for prediction of Alzheimer's disease. Neurosci Lett, 2003. 352(1): p. 67–9. [PubMed: 14615052]

4. Flood DG, Marek GJ, and Williams M, Developing predictive CSF biomarkers-a challenge critical to success in Alzheimer's disease and neuropsychiatric translational medicine. Biochem Pharmacol, 2011. 81(12): p. 1422–34. [PubMed: 21295552]

5. Veitch DP, et al. , Understanding disease progression and improving Alzheimer's disease clinical trials: Recent highlights from the Alzheimer's Disease Neuroimaging Initiative. Alzheimers Dement, 2019. 15(1): p. 106–152. [PubMed: 30321505]

6. Theurey P, et al. , Systems biology identifies preserved integrity but impaired metabolism of mitochondria due to a glycolytic defect in Alzheimer's disease neurons. Aging Cell, 2019. 18(3): p. e12924.

7. McQuade A. and Blurton-Jones M, Microglia in Alzheimer's Disease: Exploring How Genetics and Phenotype Influence Risk. J Mol Biol, 2019. 431(9): p. 1805–1817. [PubMed: 30738892]

8. Kim M, et al. , Primary fatty amides in plasma associated with brain amyloid burden, hippocampal volume, and memory in the European Medical Information Framework for Alzheimer's Disease biomarker discovery cohort. Alzheimers Dement, 2019.

9. Oresic M, et al. , Metabolome in progression to Alzheimer's disease. Transl Psychiatry, 2011. 1: p. e57.

10. Swain-Lenz D, et al. , Causal Genetic Variation Underlying Metabolome Differences. Genetics, 2017. 206(4): p. 2199–2206. [PubMed: 28652377]

11. Ganeshan K. and Chawla A, Metabolic regulation of immune responses. Annu Rev Immunol, 2014. 32: p. 609–34. [PubMed: 24655299]

12. Zhao X, et al. , Response of Gut Microbiota to Metabolite Changes Induced by Endurance Exercise. Front Microbiol, 2018. 9: p. 765. [PubMed: 29731746]

13. Fujisaka S, et al. , Diet, Genetics, and the Gut Microbiome Drive Dynamic Changes in Plasma Metabolites. Cell Rep, 2018. 22(11): p. 3072–3086. [PubMed: 29539432]

14. Mapstone M, et al. , Plasma phospholipids identify antecedent memory impairment in older adults. Nat Med, 2014. 20(4): p. 415–8. [PubMed: 24608097]

15. Han X, et al. , Metabolomics in early Alzheimer's disease: identification of altered plasma sphingolipidome using shotgun lipidomics. PLoS One, 2011. 6(7): p. e21643.

16. Barupal DK, et al. , Sets of coregulated serum lipids are associated with Alzheimer's disease pathophysiology. Alzheimers Dement (Amst), 2019. 11: p. 619–627. [PubMed: 31517024]

17. Barupal DK, et al. , Generation and quality control of lipidomics data for the alzheimer's disease neuroimaging initiative cohort. Sci Data, 2018. 5(1): p. 180263.

18. Toledo JB, et al. , Metabolic network failures in Alzheimer's disease: A biochemical road map. Alzheimers Dement, 2017. 13(9): p. 965–984. [PubMed: 28341160]

19. Varma VR, et al. , Brain and blood metabolite signatures of pathology and progression in Alzheimer disease: A targeted metabolomics study. PLoS Med, 2018. 15(1): p. e1002482.

20. Wilkins JM and Trushina E, Application of Metabolomics in Alzheimer's Disease. Front Neurol, 2017. 8: p. 719. [PubMed: 29375465]

21. Stamate D, et al. , A metabolite-based machine learning approach to diagnose Alzheimer-type dementia in blood: Results from the European Medical Information Framework for Alzheimer disease biomarker discovery cohort. Alzheimers Dement (N Y), 2019. 5: p. 933–938. [PubMed: 31890857]

22. Zhu J, et al. , Increasing the Power to Detect Causal Associations by Combining Genotypic and Expression Data in Segregating Populations. PLoS Comput Biol, 2007. 3(4): p. e69.

23. Zhu J, et al. , Integrating large-scale functional genomic data to dissect the complexity of yeast regulatory networks. Nat Genet, 2008. 40(7): p. 854–61. [PubMed: 18552845]

24. Haure-Mirande JV, et al. , Integrative approach to sporadic Alzheimer's disease: deficiency of TYROBP in cerebral Abeta amyloidosis mouse normalizes clinical phenotype and complement subnetwork molecular pathology without reducing Abeta burden. Mol Psychiatry, 2019. 24(3): p. 431–446. [PubMed: 30283032]

25. Yang X, et al. , Validation of candidate causal genes for obesity that affect shared metabolic pathways and networks. Nat Genet, 2009. 41(4): p. 415–23. [PubMed: 19270708]

26. Zhang B, et al. , Integrated systems approach identifies genetic nodes and networks in late-onset Alzheimer's disease. Cell, 2013. 153(3): p. 707–20. [PubMed: 23622250]

27. Wang M, et al. , Transformative Network Modeling of Multi-omics Data Reveals Detailed Circuits, Key Regulators, and Potential Therapeutics for Alzheimer's Disease. Neuron, 2020.

28. Beckmann ND, et al. , Multiscale causal networks identify VGF as a key regulator of Alzheimer's disease. Nat Commun, 2020. 11(1): p. 3942. [PubMed: 32770063]

29. Wang IM, et al. , Systems analysis of eleven rodent disease models reveals an inflammatome signature and key drivers. Mol Syst Biol, 2012. 8: p. 594. [PubMed: 22806142]

30. Zhong LP, et al. , Increased expression of Annexin A2 in oral squamous cell carcinoma. Arch Oral Biol, 2009. 54(1): p. 17–25. [PubMed: 18822406]

31. Zhu J, et al. , Characterizing dynamic changes in the human blood transcriptional network. PLoS Comput Biol, 2010. 6(2): p. e1000671.

32. Redestig H. and Costa IG, Detection and interpretation of metabolite-transcript coresponses using combined profiling data. Bioinformatics, 2011. 27(13): p. i357–65. [PubMed: 21685093]

33. Lempp M, et al. , Systematic identification of metabolites controlling gene expression in E. coli. Nat Commun, 2019. 10(1): p. 4463. [PubMed: 31578326]

34. Chubukov V, et al. , Coordination of microbial metabolism. Nat Rev Microbiol, 2014. 12(5): p. 327–40. [PubMed: 24658329]

35. Browning DF and Busby SJ, Local and global regulation of transcription initiation in bacteria. Nat Rev Microbiol, 2016. 14(10): p. 638–50. [PubMed: 27498839]

36. Jozefczuk S, et al. , Metabolomic and transcriptomic stress response of Escherichia coli. Mol Syst Biol, 2010. 6: p. 364. [PubMed: 20461071]

37. Donatti A, et al. , Circulating Metabolites as Potential Biomarkers for Neurological Disorders-Metabolites in Neurological Disorders. Metabolites, 2020. 10(10).

38. Kori M, et al. , Metabolic Biomarkers and Neurodegeneration: A Pathway Enrichment Analysis of Alzheimer's Disease, Parkinson's Disease, and Amyotrophic Lateral Sclerosis. OMICS, 2016. 20(11): p. 645–661. [PubMed: 27828769]

39. Pahnke J, Langer O, and Krohn M, Alzheimer's and ABC transporters--new opportunities for diagnostics and treatment. Neurobiol Dis, 2014. 72 Pt A: p. 54–60. [PubMed: 24746857]

40. Schumacher T, et al. , ABC transporters B1, C1 and G2 differentially regulate neuroregeneration in mice. PLoS One, 2012. 7(4): p. e35613.

41. Havelund JF, et al. , Biomarker Research in Parkinson's Disease Using Metabolite Profiling. Metabolites, 2017. 7(3).

42. Schipper HM and Song W, A heme oxygenase-1 transducer model of degenerative and developmental brain disorders. Int J Mol Sci, 2015. 16(3): p. 5400–19. [PubMed: 25761244]

43. LeWitt PA, et al. , Metabolomic biomarkers as strong correlates of Parkinson disease progression. Neurology, 2017. 88(9): p. 862–869. [PubMed: 28179471]

44. Costa AC, et al. , Three plasma metabolites in elderly patients differentiate mild cognitive impairment and Alzheimer's disease: a pilot study. Eur Arch Psychiatry Clin Neurosci, 2020. 270(4): p. 483–488. [PubMed: 31218445]

45. Street K, et al. , Slingshot: cell lineage and pseudotime inference for single-cell transcriptomics. BMC Genomics, 2018. 19(1): p. 477. [PubMed: 29914354]

46. Newgard CB, Interplay between lipids and branched-chain amino acids in development of insulin resistance. Cell Metab, 2012. 15(5): p. 606–14. [PubMed: 22560213]

47. Shin AC, et al. , Brain insulin lowers circulating BCAA levels by inducing hepatic BCAA catabolism. Cell Metab, 2014. 20(5): p. 898–909. [PubMed: 25307860]

48. Chen S, et al. , Effect of Allium macrostemon on a rat model of depression studied by using plasma lipid and acylcarnitine profiles from liquid chromatography/mass spectrometry. J Pharm Biomed Anal, 2014. 89: p. 122–9. [PubMed: 24284228]

49. Ahmed AT, et al. , Acylcarnitine metabolomic profiles inform clinically-defined major depressive phenotypes. J Affect Disord, 2020. 264: p. 90–97. [PubMed: 32056779]

50. St John-Williams L, et al. , Targeted metabolomics and medication classification data from participants in the ADNI1 cohort. Sci Data, 2017. 4: p. 170140.

51. St John-Williams L, et al. , Bile acids targeted metabolomics and medication classification data in the ADNI1 and ADNIGO/2 cohorts. Sci Data, 2019. 6(1): p. 212. [PubMed: 31624257]

52. Bennett DA, et al. , Religious Orders Study and Rush Memory and Aging Project. J Alzheimers Dis, 2018. 64(s1): p. S161–S189. [PubMed: 29865057]

53. Snowden SG, et al. , Association between fatty acid metabolism in the brain and Alzheimer disease neuropathology and cognitive performance: A nontargeted metabolomic study. PLoS Med, 2017. 14(3): p. e1002266.

54. Song WM and Zhang B, Multiscale Embedded Gene Co-expression Network Analysis. PLoS Comput Biol, 2015. 11(11): p. e1004574.

55. Johnson JK, et al. , Longitudinal change in neuropsychological performance using latent growth models: a study of mild cognitive impairment. Brain Imaging Behav, 2012. 6(4): p. 540–50. [PubMed: 22562439]

56. Crane PK, et al. , Development and assessment of a composite score for memory in the Alzheimer's Disease Neuroimaging Initiative (ADNI). Brain Imaging Behav, 2012. 6(4): p. 502–16. [PubMed: 22782295]

57. Swinford CG, et al. , Memory concerns in the early Alzheimer's disease prodrome: Regional association with tau deposition. Alzheimers Dement (Amst), 2018. 10: p. 322–331. [PubMed: 29780876]

58. Trzepacz PT, et al. , Relationship between the Montreal Cognitive Assessment and Mini-mental State Examination for assessment of mild cognitive impairment in older adults. BMC Geriatr, 2015. 15: p. 107. [PubMed: 26346644]

59. Saykin AJ, et al. , Genetic studies of quantitative MCI and AD phenotypes in ADNI: Progress, opportunities, and plans. Alzheimers Dement, 2015. 11(7): p. 792–814. [PubMed: 26194313]

60. Wang M, et al. , The Mount Sinai cohort of large-scale genomic, transcriptomic and proteomic data in Alzheimer's disease. Scientific Data, 2018. 5: p. 180185. [PubMed: 30204156]

61. David AB, et al. , Overview and Findings from the Religious Orders Study. Current Alzheimer Research, 2012. 9(6): p. 628–645. [PubMed: 22471860]

62. David AB, et al. , Overview and Findings from the Rush Memory and Aging Project. Current Alzheimer Research, 2012. 9(6): p. 646–663. [PubMed: 22471867]

63. Allen M, et al. , Human whole genome genotype and transcriptome data for Alzheimer's and other neurodegenerative diseases. Scientific data, 2016. 3: p. 160089.

64. Wang M, et al. , Integrative Network Analysis of Nineteen Brain Regions Identifies Molecular Signatures and Networks Underlying Selective Regional Vulnerability to Alzheimer's Disease. Genome Medicine, 2016. 8: p. 104. [PubMed: 27799057]

65. De Jager PL, et al. , A multi-omic atlas of the human frontal cortex for aging and Alzheimer's disease research. Scientific Data, 2018. 5: p. 180142.

66. Wang M, et al. , The Mount Sinai cohort of large-scale genomic, transcriptomic and proteomic data in Alzheimer's disease. Sci Data, 2018. 5: p. 180185.

67. Kim S, et al. , Influence of genetic variation on plasma protein levels in older adults using a multi-analyte panel. PLoS One, 2013. 8(7): p. e70269.

68. Zhu Z, et al. , Integration of summary data from GWAS and eQTL studies predicts complex trait gene targets. Nat Genet, 2016. 48(5): p. 481–7. [PubMed: 27019110]

69. Wu Y, et al. , Integrative analysis of omics summary data reveals putative mechanisms underlying complex traits. Nat Commun, 2018. 9(1): p. 918. [PubMed: 29500431]

70. Consortium GT, et al. , Genetic effects on gene expression across human tissues. Nature, 2017. 550(7675): p. 204–213. [PubMed: 29022597]

71. Qi T, et al. , Identifying gene targets for brain-related traits using transcriptomic and methylomic data from blood. Nat Commun, 2018. 9(1): p. 2282. [PubMed: 29891976]

72. Garnier S, et al. , Genome-wide haplotype analysis of cis expression quantitative trait loci in monocytes. PLoS Genet, 2013. 9(1): p. e1003240.

73. Huang KL, et al. , A common haplotype lowers PU.1 expression in myeloid cells and delays onset of Alzheimer's disease. Nat Neurosci, 2017. 20(8): p. 1052–1061. [PubMed: 28628103]

74. Võsa U, et al. , Unraveling the polygenic architecture of complex traits using blood eQTL metaanalysis. bioRxiv, 2018: p. 447367.

75. Arnold M, et al. , Sex and APOE epsilon4 genotype modify the Alzheimer's disease serum metabolome. Nat Commun, 2020. 11(1): p. 1148. [PubMed: 32123170]

76. Jacobs BM, et al. , Summary-data-based Mendelian randomization prioritizes potential druggable targets for multiple sclerosis. Brain Commun, 2020. 2(2): p. fcaa119.

77. Giambartolomei C, et al. , Bayesian test for colocalisation between pairs of genetic association studies using summary statistics. PLoS Genet, 2014. 10(5): p. e1004383.

78. Ramsay RR, Gandour RD, and van der Leij FR, Molecular enzymology of carnitine transfer and transport. Biochim Biophys Acta, 2001. 1546(1): p. 21–43. [PubMed: 11257506]

79. Vaz FM and Wanders RJ, Carnitine biosynthesis in mammals. Biochem J, 2002. 361(Pt 3): p. 417–29. [PubMed: 11802770]

80. Schooneman MG, et al. , Acylcarnitines: reflecting or inflicting insulin resistance? Diabetes, 2013. 62(1): p. 1–8. [PubMed: 23258903]

81. Virmani A, et al. , The Carnitine Palmitoyl Transferase (CPT) System and Possible Relevance for Neuropsychiatric and Neurological Conditions. Mol Neurobiol, 2015. 52(2): p. 826–36. [PubMed: 26041663]

82. Mihalik SJ, et al. , Increased levels of plasma acylcarnitines in obesity and type 2 diabetes and identification of a marker of glucolipotoxicity. Obesity (Silver Spring), 2010. 18(9): p. 1695–700. [PubMed: 20111019]

83. Yvan-Charvet L, et al. , ATP-binding cassette transporters and HDL suppress hematopoietic stem cell proliferation. Science, 2010. 328(5986): p. 1689–93. [PubMed: 20488992]

84. Wang N, et al. , Specific binding of ApoA-I, enhanced cholesterol efflux, and altered plasma membrane morphology in cells expressing ABC1. J Biol Chem, 2000. 275(42): p. 33053–8. [PubMed: 10918065]

85. Wang N, et al. , ATP-binding cassette transporters G1 and G4 mediate cellular cholesterol efflux to high-density lipoproteins. Proc Natl Acad Sci U S A, 2004. 101(26): p. 9774–9. [PubMed: 15210959]

86. Ganda A, et al. , Plasma metabolite profiles, cellular cholesterol efflux, and non-traditional cardiovascular risk in patients with CKD. J Mol Cell Cardiol, 2017. 112: p. 114–122. [PubMed: 28478047]

87. Kim WS, et al. , Increased ATP-binding cassette transporter A1 expression in Alzheimer's disease hippocampal neurons. J Alzheimers Dis, 2010. 21(1): p. 193–205. [PubMed: 20413849]

88. Nordestgaard LT, et al. , Loss-of-function mutation in ABCA1 and risk of Alzheimer's disease and cerebrovascular disease. Alzheimers Dement, 2015. 11(12): p. 1430–1438. [PubMed: 26079414]

89. Wolf A, Bauer B, and Hartz AM, ABC Transporters and the Alzheimer's Disease Enigma. Front Psychiatry, 2012. 3: p. 54. [PubMed: 22675311]

90. Chace DH, Kalas TA, and Naylor EW, Use of tandem mass spectrometry for multianalyte screening of dried blood specimens from newborns. Clin Chem, 2003. 49(11): p. 1797–817. [PubMed: 14578311]

91. Cristofano A, et al. , Serum Levels of Acyl-Carnitines along the Continuum from Normal to Alzheimer's Dementia. PLoS One, 2016. 11(5): p. e0155694.

92. Liang B, et al. , Adiponectin upregulates ABCA1 expression through liver X receptor alpha signaling pathway in RAW 264.7 macrophages. Int J Clin Exp Pathol, 2015. 8(1): p. 450–7. [PubMed: 25755733]

93. Liu Y. and Tang C, Regulation of ABCA1 functions by signaling pathways. Biochim Biophys Acta, 2012. 1821(3): p. 522–9. [PubMed: 21920460]

94. Koldamova R, Fitz NF, and Lefterov I, ATP-binding cassette transporter A1: from metabolism to neurodegeneration. Neurobiol Dis, 2014. 72 Pt A: p. 13–21. [PubMed: 24844148]

95. Cramer PE, et al. , ApoE-directed therapeutics rapidly clear beta-amyloid and reverse deficits in AD mouse models. Science, 2012. 335(6075): p. 1503–6. [PubMed: 22323736]

96. Price AR, et al. , Comment on "ApoE-directed therapeutics rapidly clear beta-amyloid and reverse deficits in AD mouse models". Science, 2013. 340(6135): p. 924-d.

97. Tesseur I, et al. , Comment on "ApoE-directed therapeutics rapidly clear beta-amyloid and reverse deficits in AD mouse models". Science, 2013. 340(6135): p. 924-e.

98. Veeraraghavalu K, et al. , Comment on "ApoE-directed therapeutics rapidly clear beta-amyloid and reverse deficits in AD mouse models". Science, 2013. 340(6135): p. 924-f.

99. O'Connor RS, et al. , The CPT1a inhibitor, etomoxir induces severe oxidative stress at commonly used concentrations. Sci Rep, 2018. 8(1): p. 6289. [PubMed: 29674640]

100. Morkholt AS, et al. , Blocking of carnitine palmitoyl transferase 1 potently reduces stress-induced depression in rat highlighting a pivotal role of lipid metabolism. Sci Rep, 2017. 7(1): p. 2158. [PubMed: 28526869]

101. Spyrou J, Gardner DK, and Harvey AJ, Metabolism Is a Key Regulator of Induced Pluripotent Stem Cell Reprogramming. Stem Cells Int, 2019. 2019: p. 7360121.

102. Penney J, Ralvenius WT, and Tsai LH, Modeling Alzheimer's disease with iPSC-derived brain cells. Mol Psychiatry, 2020. 25(1): p. 148–167. [PubMed: 31391546]

103. Lin Z, et al. , Fatty acid oxidation promotes reprogramming by enhancing oxidative phosphorylation and inhibiting protein kinase C. Stem Cell Res Ther, 2018. 9(1): p. 47. [PubMed: 29482657]

104. McKinney CE, Using induced pluripotent stem cells derived neurons to model brain diseases. Neural Regen Res, 2017. 12(7): p. 1062–1067. [PubMed: 28852383]

105. Tasaki S, et al. , The Molecular and Neuropathological Consequences of Genetic Risk for Alzheimer's Dementia. Front Neurosci, 2018. 12: p. 699. [PubMed: 30349450]

106. Tan CH, et al. , Polygenic hazard score, amyloid deposition and Alzheimer's neurodegeneration. Brain, 2019. 142(2): p. 460–470. [PubMed: 30689776]

107. Tan CH, et al. , Polygenic hazard score: an enrichment marker for Alzheimer's associated amyloid and tau deposition. Acta Neuropathol, 2018. 135(1): p. 85–93. [PubMed: 29177679]

108. de Haan W, et al. , ABCA1 in adipocytes regulates adipose tissue lipid content, glucose tolerance, and insulin sensitivity. J Lipid Res, 2014. 55(3): p. 516–23. [PubMed: 24443560]

109. Oku H, et al. , Adiponectin deficiency suppresses ABCA1 expression and ApoA-I synthesis in the liver. FEBS Lett, 2007. 581(26): p. 5029–33. [PubMed: 17936760]

110. Letra L, et al. , Adiponectin and sporadic Alzheimer's disease: Clinical and molecular links. Front Neuroendocrinol, 2019. 52: p. 1–11. [PubMed: 29038028]

111. Song J. and Lee JE, Adiponectin as a new paradigm for approaching Alzheimer's disease. Anat Cell Biol, 2013. 46(4): p. 229–34. [PubMed: 24386594]

112. Chan KH, et al. , Adiponectin is protective against oxidative stress induced cytotoxicity in amyloid-beta neurotoxicity. PLoS One, 2012. 7(12): p. e52354.

113. Reger MA, et al. , Intranasal insulin improves cognition and modulates beta-amyloid in early AD. Neurology, 2008. 70(6): p. 440–8. [PubMed: 17942819]
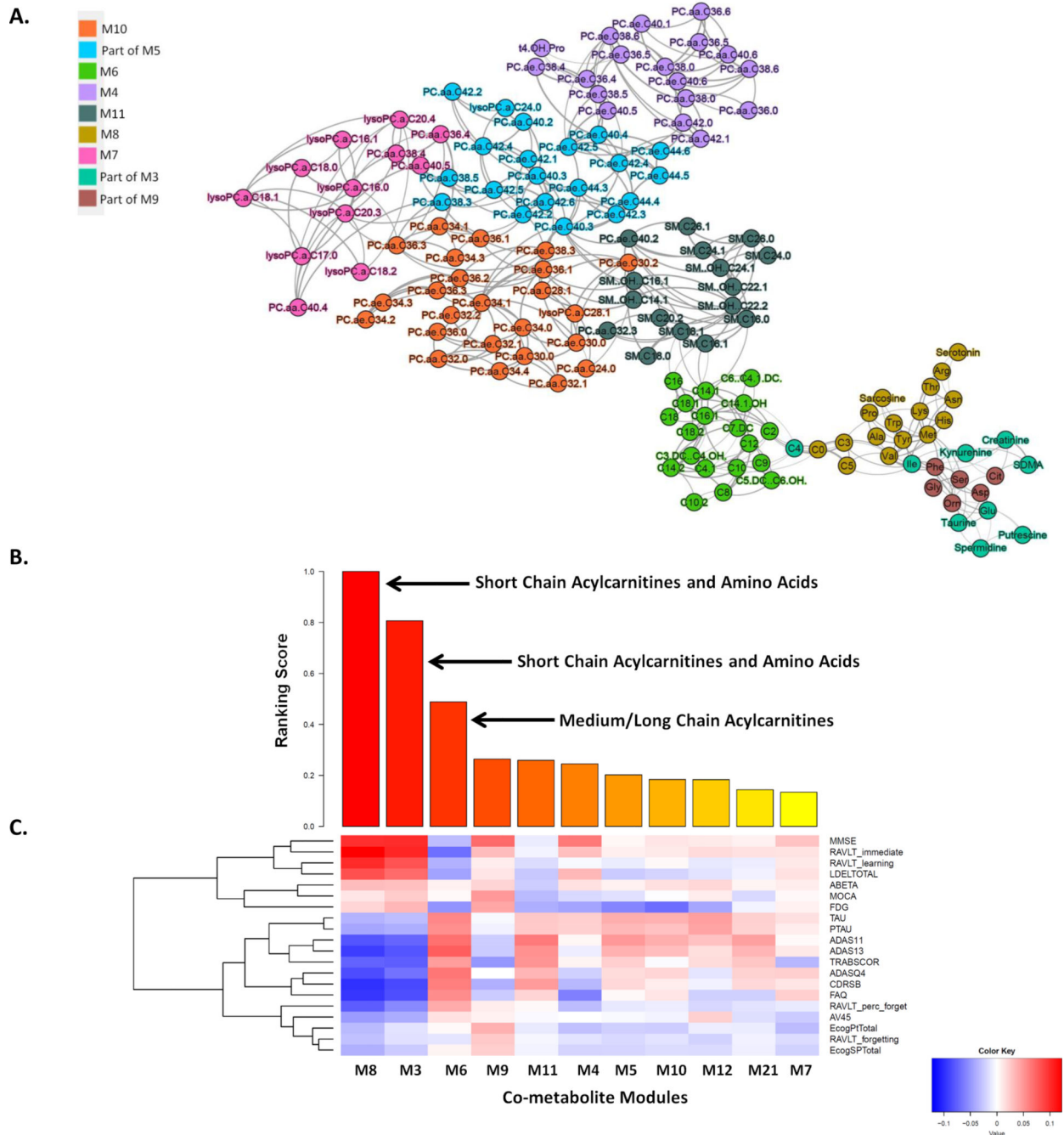
A.

B.

C.

Figure 1. Multiscale metabolite co-expression network analysis of the blood metabolomic data in the ADNI.
(A) The global metabolite co-expression network. Two parent modules M3 and M5 are not shown here. (B) Rank-ordered metabolite modules by the extent of association to the clinical outcomes. (C) Heatmap of the correlations between clinical/cognitive AD-pathology related traits and metabolite modules. Cognitive and pathological traits are shown on the right axis while the metabolite modules are shown at the bottom axis. The intensity of the color in each cell indicates the magnitude of the Spearman's rank correlation coefficient between

the corresponding row and column variables, for those correlations with adjusted p values <0.05. Red and blue colors indicate positive and negative correlations, respectively.
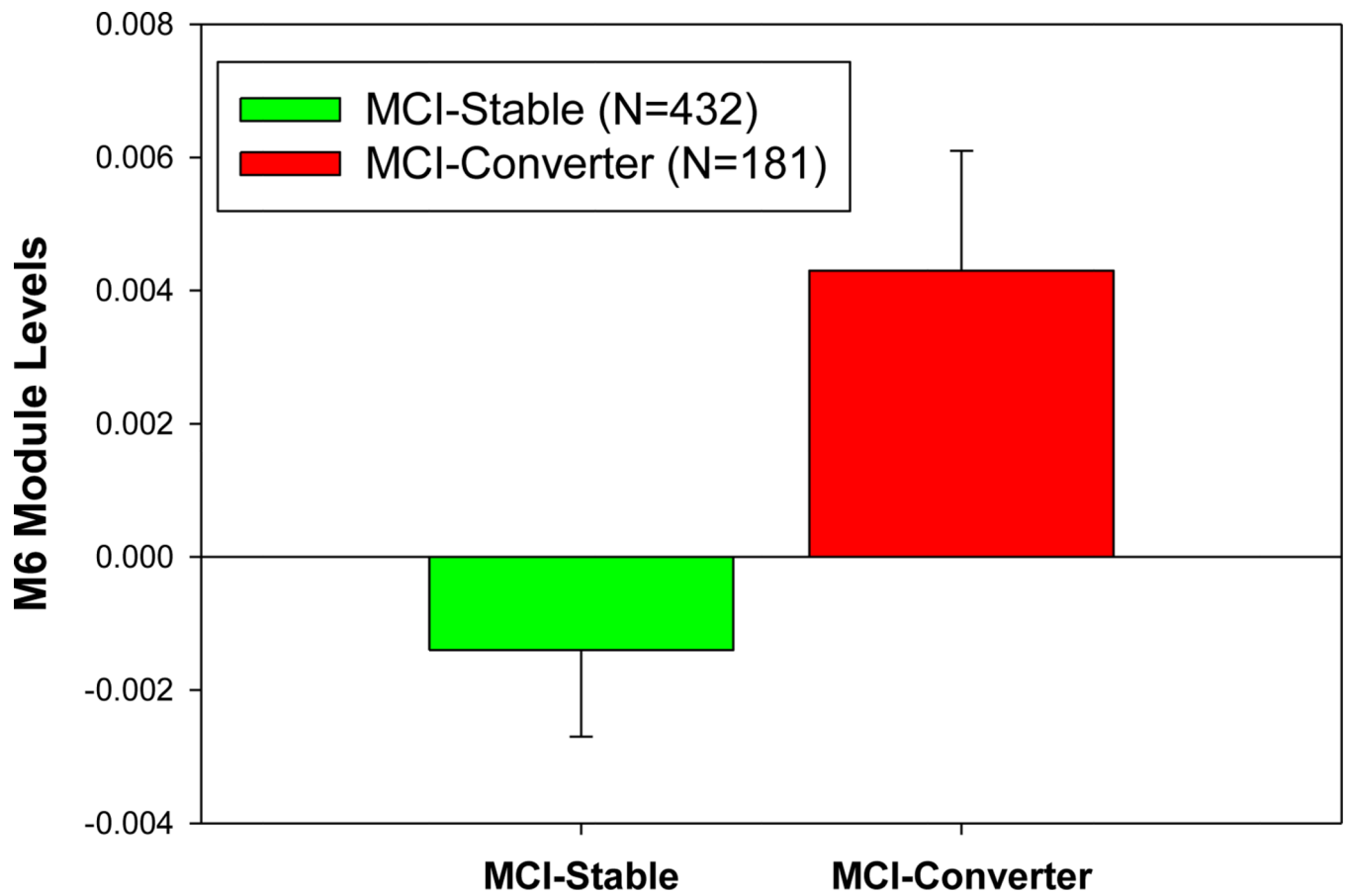
Figure 2.
The expression level of the module M6 (i.e., module eigen-metabolite represented by the first PC of the module) significantly increases in the subjects with conversion from MCI to AD (termed MCI converters) compared with those MCI subjects without conversion (termed MCI stable group) in two years.

Figure 3. *CPT1A* centered co-expression networks.
(A) The genes positively correlated with *CPT1A* (FDR $< 10^{-6}$). (B) MSigDB GO and canonical pathways enriched in the *CPT1A* centered subnetwork shown in (A). (C) The genes negatively correlated with CPT1A (FDR $< 10^{-6}$). (D) MSigDB GO and canonical pathways enriched in the *CPT1A* centered subnetwork shown in (C). The blue bars represent the –log10 values of the adjusted p-values.
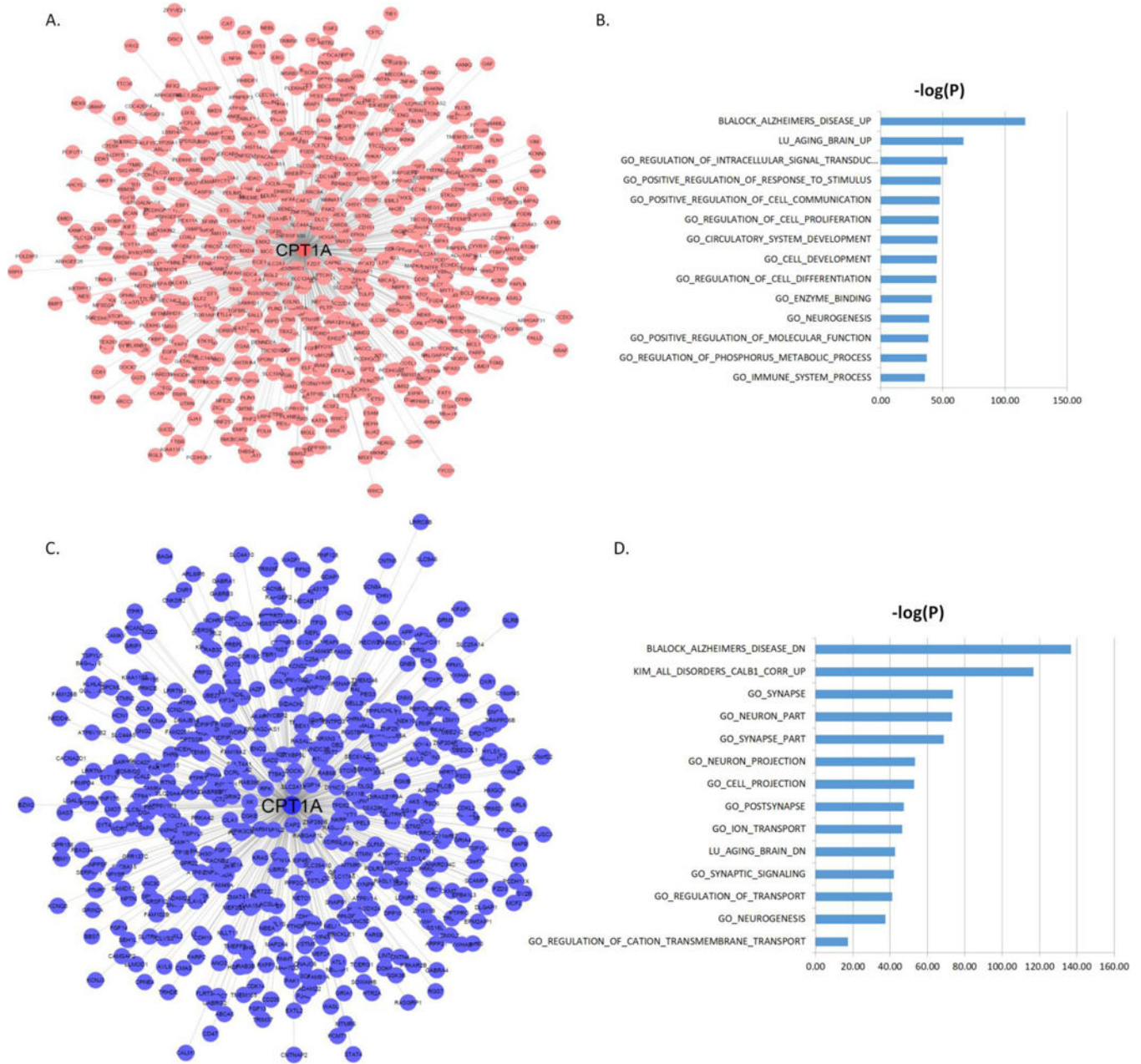
Figure 4. *ABCA1* centered co-expression networks.
(A) The genes positively correlated with *ABCA1* (FDR < 10^{-6}). (B) MSigDB GO and canonical pathways enriched in the *ABCA1* centered subnetwork shown in (A). (C) The genes negatively correlated with *ABCA1* (FDR < 10^{-6}). (D) MSigDB GO and canonical pathways enriched in the *ABCA1* centered subnetwork shown in (C). The blue bars represent the –log10 values of the adjusted p-values.
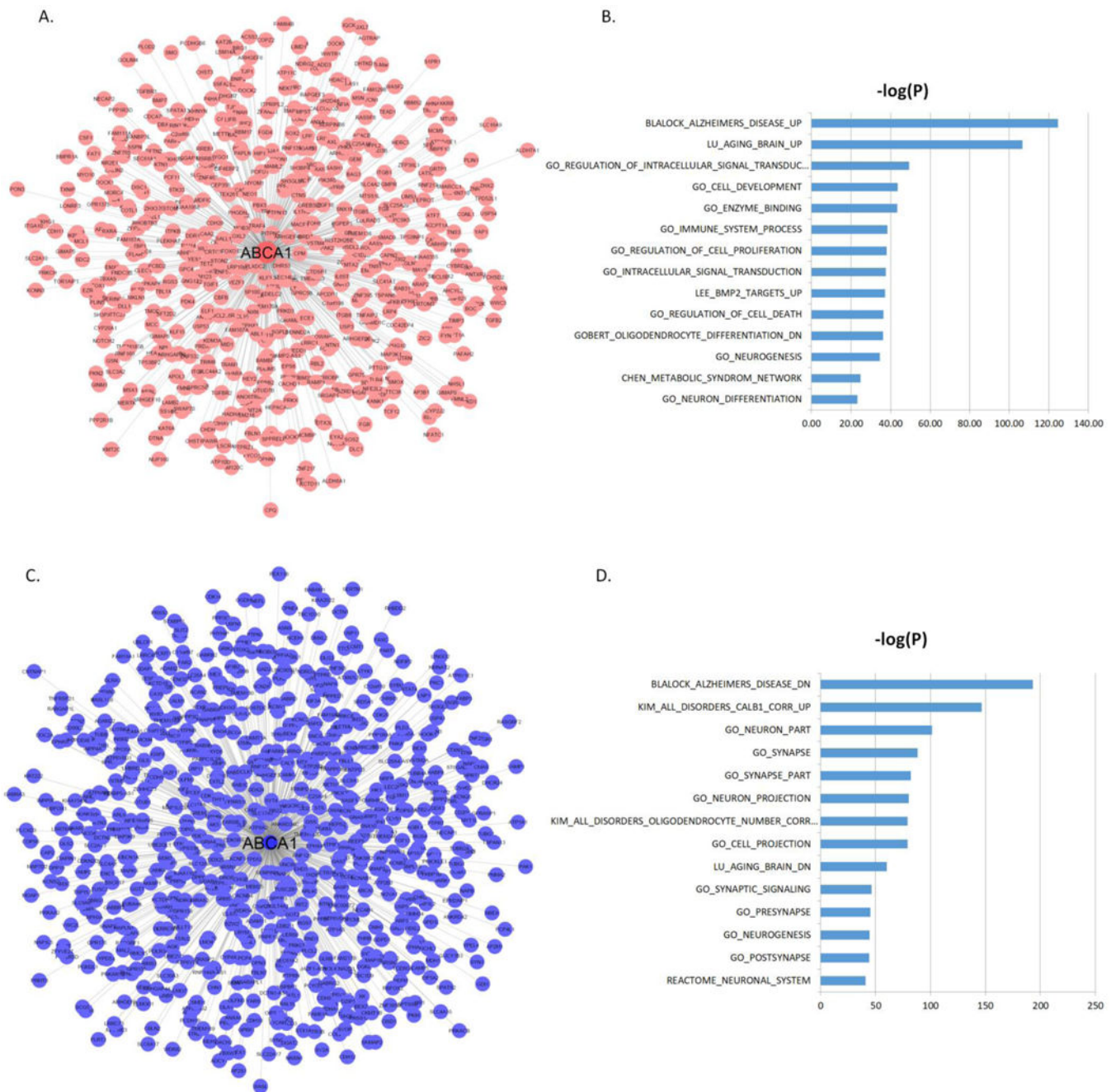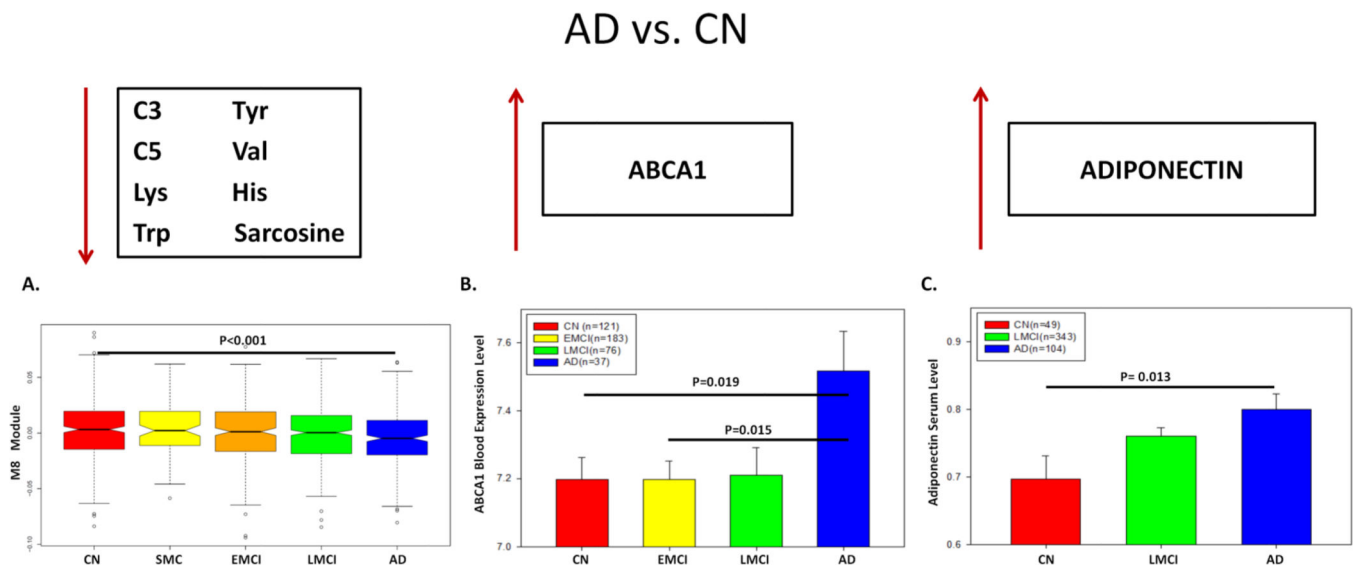
Figure 5. Integrative analysis of metabolites, genes and proteins.
(A) The expression level of the module M8 (i.e., the eigen-metabolite represented by the first PC of the module), which contains short-chain acylcarnitine and amino acid, varies significantly across five diagnosis groups (p-value < 0.05). (B) *ABCA1* mRNA level in the blood is significantly different across four diagnosis groups. (C) Adiponectin protein level in the blood is significantly different across AD, LMCI and control.

Figure 6. Medium/long chain acylcarnitines are significantly associated with NGAL protein level in AD.

(A) Medium/long-chain acylcarnitines module (M6) expression level increases during the disease progression from control to LMCI and to AD. (B) NGAL protein level in blood is significantly different across diagnosis groups (p-value < 0.05).
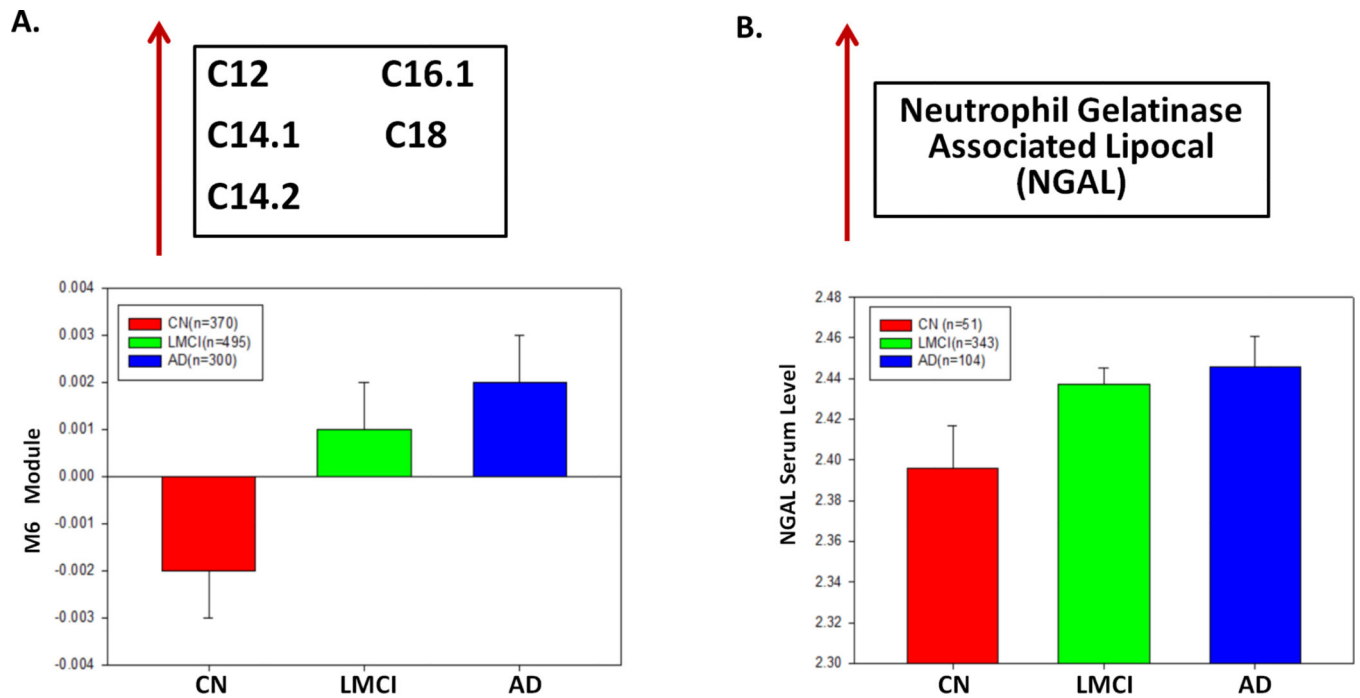
Table 1.

Pearson correlation analysis of the top three modules (including acylcarnitines and amino acids) and the blood gene expression data in ADNI. The module M6 includes medium/long-chain acylcarnitines while the modules M8 and M3 include short-chain acylcarnitines and amino acids, respectively.

Gene Expression (N=17849)	Top Metabolite Modules	Rho value	p-value	p.adj
CPT1A (Carnitine Palmitoyltransferase 1A)	M6	0.317	3.50×10^{-11}	1.87×10^{-6}
SLC25A20 (Carnitine/Acylcarnitine Translocase)	M6	0.261	6.60×10^{-8}	1.8×10^{-3}
ABCA1 (ATP Binding Cassette Subfamily A Member 1)	M8	−0.236	1.10×10^{-6}	0.02
MRPL47	M3	0.233	1.50×10^{-6}	0.02
ABCA1	M3	−0.23	2.10×10^{-6}	0.02
ABCG1	M3	−0.222	4.90×10^{-6}	0.038
PDK4	M6	0.222	4.60×10^{-6}	0.038
UCHL3	M3	0.22	5.80×10^{-6}	0.039
CCT2	M3	0.215	9.10×10^{-6}	0.049
ABCG1	M8	−0.216	8.80×10^{-6}	0.049

Table 2.

Differentially expressed genes in the human brain from the MSBB cohort. logFC= fold change; Padj = FDR adjusted p-value; AD = Alzheimer's Disease; CN = Cognitively Normal.

Gene	logFC	p-value	Padj	Contrast	Region
CPT1A	0.27	9.09×10^{-6}	1.61×10^{-4}	AD vs CN	PHG
ABCA1	0.41	2.56×10^{-6}	7.53×10^{-5}	AD vs CN	PHG
CPT1A	0.39	1.15×10^{-5}	3.06×10^{-4}	AD vs CN	TCX
ABCA1	0.56	3×10^{-6}	1.35×10^{-4}	AD vs CN	TCX

Table 3:

The top 10 proteins most correlated with the top AD associated metabolite modules which include acylcarnitines and amino acids.

Protein	Top Modules	Rho value	P-value	P.adj
Adiponectin..ug.mL.	**M3**	**−0.168**	**0.00017**	**0.01241**
Adiponectin..ug.mL.	**M8**	**−0.165**	**0.00022**	**0.012653**
Hepatocyte Growth Factor..HGF…ng.mL.	M6	0.225	4.20×10^{-7}	0.000173
Neutrophil.Gelatinase.Associated.Lipocal..ng.ml.	**M6**	**0.22**	**7.90×10^{-7}**	**0.000173**
Thrombomodulin..TM…ng.ml.	M6	0.188	2.60×10^{-5}	0.003614
Myoglobin..ng.mL.	M6	0.185	3.30×10^{-5}	0.003614
Chemokine.CC.4..HCC.4…ng.mL.	M6	0.17	0.00014	0.012264
FASLG.Receptor..FAS…ng.mL.	M6	0.163	0.00026	0.012653
Myeloid.Progenitor.Inhibitory.Factor.1….ng.mL.	M6	0.163	0.00026	0.012653
Cystatin.C..ng.ml.	M6	0.162	0.00029	0.012702
CD.40.antigen..CD40…ng.mL.	M6	0.159	0.00039	0.015529
Beta.2.Microglobulin..B2M…ug.mL.	M6	0.154	0.00059	0.019436
Thymus.Expressed.Chemokine..TECK…ng.mL.	M6	0.153	0.00063	0.019436
Ferritin..FRTN…ng.mL.	M6	0.152	0.00067	0.019436
AXL.Receptor.Tyrosine.Kinase..AXL…ng.mL.	M6	0.151	0.00071	0.019436
Vascular.Cell.Adhesion.Molecule.1..VCAM…ng.mL.	M6	0.152	0.00071	0.019436
Brain.Natriuretic.Peptide…BNP…pg.ml.	M6	0.147	0.0011	0.028341
Pancreatic.Polypeptide..PPP…pg.ml.	M6	0.141	0.0016	0.038933
B.Lymphocyte.Chemoattractant..BLC…pg.ml.	M6	0.14	0.0018	0.041495